JACS
JOURNAL OF THE AMERICAN CHEMICAL SOCIETY

Article

pubs.acs.org/JACS

NMR Studies of Protonation and Hydrogen Bond States of Internal Aldimines of Pyridoxal 5′-Phosphate Acid−Base in Alanine Racemase, Aspartate Aminotransferase, and Poly-L-lysine

Monique Chan-Huot,*[,†,‡] Alexandra Dos,[†] Reinhard Zander,[†] Shasad Sharif,[†] Peter M. Tolstoy,[†,§] Shara Compton,[∥,⊥] Emily Fogle,[∥,#] Michael D. Toney,[∥] Ilya Shenderovich,[†,+] Gleb S. Denisov,[○] and Hans-Heinrich Limbach*[,†]

[†]Institut für Chemie und Biochemie, Freie Universität Berlin, Takustr. 3, 14195 Berlin, Germany

[‡]Ecole Normale Supérieure, Laboratoire des BioMolécules, 24 rue Lhomond, 75231 Cedex 05, Paris, France

[§]Department of Chemistry, St. Petersburg State University, Universitetskij pr. 26, 198504 St. Petersburg, Russian Federation

[∥]Department of Chemistry, University of California—Davis, One Shields Avenue, Davis, California 95616, United States

[⊥]Department of Chemistry, Widener University, One University Place, Chester, Pennsylvania 19013, United States

[#]Department of Chemistry & Biochemistry, CalPoly, San Luis Obispo, California 93407, United States

[+]University of Regensburg, Universitätsstr. 31, 93040 Regensburg, Germany

[○]Institute of Physics, St. Petersburg State University, 198504 St. Petersburg, Russian Federation

Supporting Information

ABSTRACT: Using ^{15}N solid-state NMR, we have studied protonation and H-bonded states of the cofactor pyridoxal 5′-phosphate (PLP) linked as an internal aldimine in alanine racemase (AlaR), aspartate aminotransferase (AspAT), and poly-L-lysine. Protonation of the pyridine nitrogen of PLP and the coupled proton transfer from the phenolic oxygen (enolimine form) to the aldimine nitrogen (ketoenamine form) is often considered to be a prerequisite to the initial step (transimination) of the enzyme-catalyzed reaction. Indeed, using ^{15}N NMR and H-bond correlations in AspAT, we observe a strong aspartate-pyridine nitrogen H-bond with H located on nitrogen. After hydration, this hydrogen bond is maintained. By contrast, in the case of solid lyophilized AlaR, we find that the pyridine nitrogen is neither protonated nor hydrogen bonded to the proximal arginine side chain. However, hydration establishes a weak hydrogen bond to pyridine. To clarify how AlaR is activated, we performed ^{13}C and ^{15}N solid-state NMR experiments on isotopically labeled PLP aldimines formed by lyophilization with poly-L-lysine. In the dry solid, only the enolimine tautomer is observed. However, a fast reversible proton transfer involving the ketoenamine tautomer is observed after treatment with either gaseous water or gaseous dry HCl. Hydrolysis requires the action of both water and HCl. The formation of an external aldimine with aspartic acid at pH 9 also produces the ketoenamine form stabilized by interaction with a second aspartic acid, probably via a H-bond to the phenolic oxygen. We postulate that O-protonation is an effectual mechanism for the activation of PLP, as is N-protonation, and that enzymes that are incapable of N-protonation employ this mechanism.

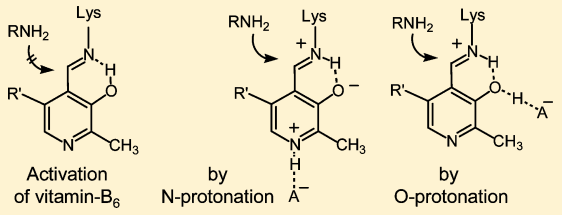

INTRODUCTION

Pyridoxal 5′-phosphate or vitamin B_6 (PLP, Scheme 1) is a metabolically central cofactor of enzymes of broad importance[1] that catalyze a variety of amine and amino acid transformations.[2−5] Because it encompasses four functional groups, PLP exists in a number of different protonation states and tautomers, which enables its biochemical functions. As illustrated in Scheme 1, in aqueous solution PLP exists as aldehyde **1a** under neutral and basic conditions or as hydrate **1h** under acidic conditions.[6] With aliphatic amino groups, it forms aldimines **1s** subject to a reversible proton tautomerism between enolimine tautomer **1s-e** and ketoenamine tautomer **1s-k** (Scheme 1). In enzymic environments, internal aldimines are formed with the ε-amino group of lysine residues in the active site. External aldimines are formed with substrate amino acids, releasing the lysine in a process called transimination (Scheme 1).[7] Evidence has been obtained from spectroscopic and kinetic studies[8−17] and from computational studies[18] for the formation of geminal diamines **1g** along the enzymic transimination pathways. Moreover, enzymic geminal diamine intermediates have been observed by X-ray crystallography,[19−25] although the protonation states of the amino nitrogens could not be determined by this method. In one case, tetrahedral adducts of enzymic PLP with water have been

Received: August 30, 2013
Published: October 22, 2013

dx.doi.org/10.1021/ja408988z | J. Am. Chem. Soc. 2013, 135, 18160−18175

Scheme 1. Main Chemical Structures of Pyridoxal 5′-Phosphate (PLP, 1) and Derivatives, Tautomerism of PLP Aldimines, and Transimination between Internal and External Aldimines

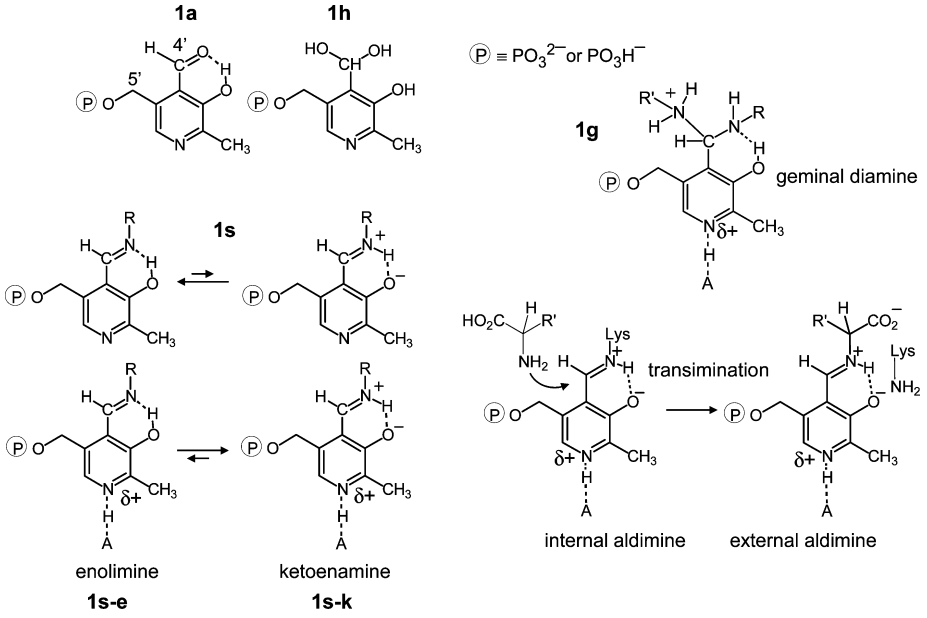

detected.[24] The latter could be intermediates of a hydrolysis mechanism that has also been discussed in the literature.[26,27]

It has been argued that the nucleophilic attack of the substrate amino group on C-4′ of the internal aldimine in the first step of transimination requires a positive charge on the aldimine nitrogen.[3,28−30] For that, the bridging proton of the intramolecular OHN hydrogen bond has to be transferred from the phenolic oxygen to the aldimine nitrogen, a process that is supposed to be facilitated by the protonation of the pyridine nitrogen.[2,29−31]

Liquid- and solid-state NMR are important techniques for studying proton transfer and H-bonding,[32,33] and some of us have used these techniques to study the protonation states of PLP and PLP aldimines in aqueous solution,[34,35] in the solid state,[36,37] and in polar aprotic solution.[38,39] Indeed, we observed cooperativity between the two OHN hydrogen bonds of model PLP aldimines.[37,39] It was found that the equilibrium constants of the enolimine−ketoenamine tautomerism are increased substantially when the pyridine nitrogen is involved in a strong H-bond or is protonated as illustrated in Scheme 1. In addition, increasing solvent polarity shifts the proton toward the pyridine nitrogen in complexes with proton donors, which in turn shifts the proton in the intramolecular OHN H-bond from the phenolic oxygen to the aldimine nitrogen.

These model studies led us to study the hydrogen bond and protonation states of the pyridine and Schiff base nitrogens of PLP directly in protein environments using combined liquid- and solid-state NMR. We focused first on *E. coli* aspartate aminotransferase (AspAT, ∼88 kDa)[31] in which PLP is covalently bound to Lys258 as an internal aldimine in the active site, as has been shown by X-ray crystallography.[40] The active-site structure is depicted schematically in Scheme 2a. In this diagram, some important hydrogen atoms that cannot be detected by X-ray crystallography are tentatively introduced in probable positions. The pyridine nitrogen atom forms an OHN hydrogen bond to the side-chain carboxylate of Asp222. An O···N distance of 2.64 Å was determined, but OH and HN

Scheme 2. Schematic Views of PLP (a) in AspAT[40b] from *E. coli* and (b) in AlaR from *Bacillus anthracis*[47a]

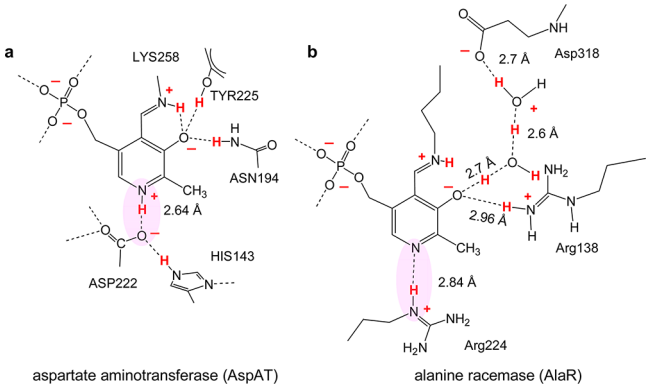

[a]Hydrogen positions and charges are tentatively introduced in plausible positions. Water oxygen positions in structure b are derived from the X-ray structure.[47]

distances could not be obtained.[40b] Removal of the carboxylate group by the D222A mutation indeed produces an inactive enzyme.[41] Pyridine ring ^{15}N-labeled PLP was synthesized and introduced into the active site of AspAT. Its protonation and hydrogen bond states were studied using high-resolution ^{15}N solid-state NMR with cross-polarization (CP) and magic angle spinning (MAS). Thus, the formation of a strong OHN hydrogen bond and a proton located near the pyridine nitrogen was confirmed for microcrystalline AspAT and the AspAT-maleate inhibitor complex.[42] This finding is noteworthy because the pK_a of the pyridine nitrogen is about 5.8[34] whereas the pK_a of an aspartic acid side chain is 3.9;[43] thus, whereas both residues are deprotonated in water at physiological pH, their ability to bind a proton cooperatively is strongly increased in the AspAT active site. An account of previous NMR work in this field has been given recently.[44]

By contrast, alanine racemase (AlaR), a potential target for antibiotics[45] that interconverts L- and D-alanine, behaves in a

dx.doi.org/10.1021/ja408988z | J. Am. Chem. Soc. 2013, 135, 18160−18175

Scheme 3. Activation of Cofactor PLP in PLP-Dependent Enzymes[a]

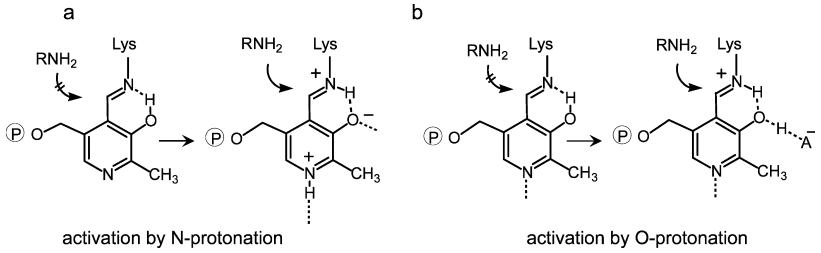

[a]Activation occurs by either (a) N-protonation, as previously proposed, or (b) O-protonation, as proposed in this study.

very different way. This enzyme is difficult to crystallize. Ringe et al.[46] crystallized AlaR from *Bacillus stearothermophilus* in the presence of acetate. The X-ray crystal structure obtained at 1.9 Å resolution showed an acetate bound in the active site near the phenolic oxygen of PLP. Au et al. crystallized AlaR from *Bacillus anthracis* without ligands or inhibitors after the reductive methylation of some of the lysine side chains and obtained a crystal structure at 1.47 Å resolution.[47] A schematic view of the active site including some important side chains, hydrogen bonds, and crystallographic water molecules derived from the crystallographic structure[47] is depicted in Scheme 2b. Instead of the acetate, a chain of two water molecules is observed in the *Bacillus anthracis* structure, which provides a link between phenolic oxygen O-3′ and the carboxylic group of Asp318. We have again tentatively added hydrogen atoms in plausible positions. To produce a hydrogen bond pattern consistent with the short O···O distance of 2.62 Å, we had to add an additional proton between the two water molecules leading to a distorted Zundel cation hydrogen bonded to two anionic oxygen atoms. The existence of the excess proton has not been discussed to our knowledge, nor has the role of this water chain and its importance to the transimination. This excess proton as well as Arg138 probably fulfills the role of neutralizing the negative charge on O-3′ and on Asp318, whereas in AspAT there is no charged residue interacting with O-3′.

One large difference between AspAT and the two AlaR structures is that in the latter the pyridine rings are involved only in weak hydrogen bonds with an arginine side chain, exhibiting N···N distances of between 2.8 and 2.9 Å.[40b,47] Because the basicity of the arginine guanidine group is much greater than that of a pyridine ring, one assumes that the pyridine ring is not protonated in AlaR. This raises the question of how PLP is activated for nucleophilic attack without pyridine ring protonation.

Before the AlaR structure from *Bacillus anthracis* was known, QM/MM studies on AlaR by Gao et al.[48] proposed that the positive charge on the Schiff base nitrogen of the ketoenamine tautomer, stabilized by local solvent dipoles, is sufficient to initiate the reaction, although the whole aldimine is neutral because of the compensating negative charge at the phenolic oxygen. However, PLP-lysine Schiff bases in the ketoenamine form are stable in water up to pH 10, and hydrolysis occurs only at higher pH.[6] NMR studies of solid external aldimines of AlaR by Griffin et al.[49] and of tryptophan synthase by Mueller et al.[50] with ^{15}N-labeled inhibitors indicated the presence of the ketoenamine form in the first case and of a fast enolimine−ketoenamine tautomerism in the second.

Because the mechanism of the transimination of AlaR is still unclear, we thought that studies of the hydrogen bond structures of AspAT and AlaR might shine new light on the activation of PLP-dependent enzymes. To determine the hydrogen bond structures in which the pyridine ring is involved, we have labeled PLP chemically with ^{15}N in the pyridine ring and introduced it into AspAT and AlaR for subsequent solid- and liquid-state ^{15}N NMR experiments. Although we could obtain AspAT microcrystals, we could not crystallize AlaR in the absence of acetate and studied lyophilized samples.

Unfortunately, the characterization of the Schiff base nitrogens of the internal aldimines by ^{15}N NMR requires a difficult, specific ^{15}N labeling of the corresponding lysine ε-amino groups. Therefore, we have used poly-L-lysine (PLL) as a protein model environment for the internal aldimines of PLP whose ε-amino groups could easily be labeled with ^{15}N. Various lyophilized solid samples containing ^{13}C and ^{15}N in different positions were prepared, allowing us to observe changes using ^{13}C and ^{15}N CPMAS NMR after adding water and/or acid. The interpretation of the results is facilitated by previous studies of protonation and H-bond states of the amino groups in PLL.[51] In addition, the ^{13}C and ^{15}N CPMAS NMR spectra of an external aldimine model system with ^{15}N-labeled aspartic acid were studied.

The working hypothesis resulting from these studies is depicted in Scheme 3, where we propose that, as an alternative to protonation or strong hydrogen bond formation to the pyridine nitrogen, protonation or strong hydrogen bond formation to the oxygen of the phenolate might activate the cofactor.

This Article is organized as follows. After an experimental section, we report the results of our solid- and liquid-state NMR studies of internal PLP aldimines in AlaR, AspAT, and poly-L-lysine. The results and their implications for the biological function of PLP are then discussed.

EXPERIMENTAL SECTION

Enzyme Purification and Cofactor Exchange. AspAT was overexpressed in *E. coli* strain DB120 (DG-70) and purified as described previously.[52] The pyridoxamine phosphate (PMP) enzyme form was obtained by adding 5 mM cysteine sulfinate on ice. The solution was stirred for 30 min, and the pH was decreased to 4.9 with glacial acetic acid. The conversion to the PMP form was followed by the loss of the bright-yellow color of enzyme-bound PLP. The PMP enzyme was then precipitated by adding ammonium sulfate to 75% saturation on ice. PMP was removed by washing the precipitate with an ice-cold solution of ammonium sulfate (4 M at 0 °C). After centrifugation, the pellets containing the apoenzyme were suspended in 50 mL of a 20 mM MOPS buffer solution titrated with bis-tris-propane to pH 7.5.

The apoenzyme was concentrated with an Amicon concentrator (Ultra-4 centrifuge from Millipore, 10 000 molecular weight cutoff) for 50 min at 18 000 rpm. The concentration of the enzyme was

dx.doi.org/10.1021/ja408988z | J. Am. Chem. Soc. 2013, 135, 18160−18175

determined by measurement of the absorbance at 205 nm. Approximately 330 mg of apoenzyme was obtained.

Isotopically labeled holoenzyme was obtained by adding 1 mol eq. of ^{15}N-PLP[34] to the solution of the apoenzyme, which became bright yellow as a result of internal aldimine formation. Microcrystallization was performed by adding dropwise a saturated solution of ammonium sulfate (2 mL) to a solution containing the holoenzyme (2 mL, 770 μM) and PLP (20 μL, 77 μM) under very slow stirring. The addition was stopped once the solution became turbid. The solution was covered with Parafilm and left in the dark overnight. The microcrystalline precipitate was centrifuged and transferred to a 4 mm rotor.

Alanine racemase from *Geobacillus stearothermophilus* was expressed in *E. coli* strain BL21 (DE3) and purified as described previously.[53] Holoalanine racemase was treated with a 10-fold molar excess of hydroxylamine, which reacts with PLP to form an oxime. The solution was then dialyzed three times against 100 mM sodium acetate, 30 mM TEA-HCl, pH 8.0, and 0.1% β-mercaptoethanol in order to obtain the apoenzyme. ^{15}N-PLP[34] was added to the apoenzyme, and the resulting solution rapidly turned yellow because of internal aldimine formation. The reconstituted AlaR was flash frozen in 2-propanol/dry ice and lyophilized. The enzyme was stored at −70 °C. The protein concentration was determined by the DC protein assay (modified Lowry) from Bio-Rad with bovine serum albumin as the standard. Hydration of the solid AlaR sample was achieved via the gas phase in a desiccator containing water. A gain of 56% in weight was obtained, corresponding to a total water content of 36%.

Syntheses. *Synthesis of $^{15}N_\varepsilon$-Poly-L-lysine.* High molecular weight poly-L-lysine (PLL_h), enriched to about 50% with the ^{15}N isotope in the amino (N_ε) side-chain positions, was synthesized as described previously[51a] by modification of the procedure of Hernandez et al.[54] The final product, PLL·HCl, exhibited a molecular weight of 160 000 ± 40 000 Da, corresponding to 1000 ± 250 monomers in the polypeptide. Low molecular weight poly-L-lysine (PLL_l) was synthesized by slight modifications of the PLL_h synthesis and was enriched to ∼98% with the ^{15}N isotope in the amino (N_ε) side-chain position. N_ε-Carboxy-anhydride-Boc-L-lysine (NCA) was prepared with triphosgene instead of phosgene, and the polymerization was induced with dry triethylamine instead of sodium methoxide as described in detail in the Supporting Information. MALDI-TOF mass spectra indicated that the final polymer contained about 19 lysine residues ($M \approx 1659$ g·mol^{-1}). The raw product was dissolved in water and dialyzed against water (5 cm tube, molecular weight cutoff 1000 g·mol^{-1}), with the water changed daily for 3 days (1 L of H_2O each time). The cleaned poly-L-lysine was then lyophilized and stored under argon in the freezer. Yield 1.06 g (starting from 910 mg of N^ε,N^ε-di(tert-butoxycarbonyl)-L-lysine and 4 g of ^{15}N-lysine).

Water was degassed prior to use and stored under argon in order to avoid carbamate formation from atmospheric CO_2 and the amino groups.[55] The pH was adjusted using a HANNA HI 9025 pH meter with a Hamilton Spintrode P electrode using sodium hydroxide and hydrochloric acid solutions in degassed water at concentrations of 3, 1, and 0.1 M.

Synthesis of ^{13}C-Enriched Pyridoxal 5′-Phosphate (PLP). PLP was isotopically enriched with 25% ^{13}C from a multistep synthesis starting from commercially available ^{13}C-enriched maleic anhydride as described previously.[35]

Preparation of Aldimines in PLL. $^{15}N_\varepsilon$-Poly-L-lysine (26 mg, 0.2 mmol) was dissolved in 15 mL of degassed water, resulting in a final concentration of 6 M. The process was assisted by an ultrasonic bath, and the initial pH was 5.8. Lyophilized ^{13}C-4′,5′-PLP (**1a**/**1h**) was added in PLP/Lys ratios of 1:1 and 1:2 to the PLL solution (50 mg, 0.2 mmol: 100 mg, 0.4 mmol). After addition, the pH of the aqueous solution dropped to 2.6. The mixture became intensively yellow because of the formation of aldimine **1s**. The pH was adjusted to 9 with sodium hydroxide. The mixture was stirred overnight and lyophilized to obtain **1s** as a yellow solid.

The pH value and the PLL concentration of the solution were held at 9.0 and 6 M, respectively, because these were the conditions under which the most aldimine **1s** was formed. (See Figures S1 and S2 in the SI for the PLL concentration and pH dependence of aldimine formation.) Some samples were lyophilized at higher pH values.

The lyophilized samples were transferred into rotors and subsequently dried further inside the uncapped rotor at room temperature under vacuum below 10^{-5} mbar. The samples were dried for 24 h and then flushed with argon. The rotors were closed with Teflon sealing caps and measured with NMR.

To hydrate the samples, the rotors were uncapped and then exposed to water vapor in a desiccator by placing a receptacle filled with water at the bottom. The mass of added water was then calculated by subtracting the mass of the rotor before hydration from the mass of the rotor after exposure to water vapor.

The number of molecules of water per aldimine unit was calculated as follows. The total number of residues n in the polymer was obtained from the sample preparation

$$n = \frac{m_{\mathrm{Lys}}}{M_{\mathrm{Lys}}} \tag{1}$$

where m_{Lys} is the initial total mass of the polymer dissolved in water. At pH 9, the amino groups are protonated, and with chloride as a counteranion, a lysine residue exhibits the molecular formula $C_6H_{13}ON_2Cl$ for which we calculate a molar mass of m_{Lys} = 164.5 g·mol^{-1}. The number of PLL-Lys aldimine residues is given by

$$n_{\mathrm{PLP\text{-}lys}} = \frac{m_{\mathrm{PLP}}}{M_{\mathrm{PLP}}} \tag{2}$$

where m_{PLP} is the initial mass of PLP dissolved. At pH 9, the phosphate of PLP is dianionic; with sodium as countercation we obtain a mass of M_{PLP} = 290 g·mol^{-1} for the molecular formula $C_8H_7O_6NPNa_2$ of unlabeled PLP aldehyde **1a**. As one water molecule is released by the formation of an aldimine, the molecular weight of a PLP-lysine residue exhibiting the molecular formula $C_{14}H_{18}O_6PN_3Na_2Cl$ is $M_{\mathrm{PLP\text{-}Lys}} = M_{\mathrm{PLP}} + M_{\mathrm{Lys}} - M_{\mathrm{H_2O}}$ = 436.5 g·mol^{-1}. Isotopic labeling with one ^{13}C or ^{15}N increases the molecular masses by 1 unit. The total mass m of the dry sample is then given by

$$m = (n - n_{\mathrm{PLP\text{-}Lys}})M_{\mathrm{lys}} + n_{\mathrm{PLP\text{-}Lys}}M_{\mathrm{PLP\text{-}Lys}} \tag{3}$$

With the molar ratio

$$R = \frac{n_{\mathrm{PLP\text{-}Lys}}}{n - n_{\mathrm{PLP\text{-}Lys}}} \tag{4}$$

we obtain

$$n_{\mathrm{PLP\text{-}Lys}} = \frac{Rm}{M_{\mathrm{lys}} + RM_{\mathrm{PLP\text{-}Lys}}} \tag{5}$$

The number of water molecules per PLP-lysine aldimine is then given by

$$\frac{n_{\mathrm{H_2O}}}{n_{\mathrm{PLP\text{-}Lys}}} = \frac{m_{\mathrm{H_2O}}(M_{\mathrm{lys}} + RM_{\mathrm{PLP\text{-}Lys}})}{M_{\mathrm{H_2O}}Rm} \tag{6}$$

The samples were exposed to gaseous HCl for 10 min in a closed apparatus with a sodium carbonate bubbler at the exit. The system was purged with argon at the end of the operation. The rotors were then immediately resealed with the Teflon caps.

Spectroscopic Methods. Solution NMR spectra were measured using a Bruker AMX 500 spectrometer (500.13 MHz for ^{1}H and 50.68 MHz for ^{15}N). Inverse gated ^{1}H-decoupled ^{15}N spectra were recorded in H_2O with field locking on a D_2O-containing capillary with a recycle delay set to 10 s and a pulse length of 11 μs on the ^{15}N channel. The ^{15}N spectra of neat nitromethane containing a D_2O capillary were recorded under the same ^{2}H field locking conditions in order to reference the ^{15}N chemical shifts. The relation δ (CH_3NO_2, liq.) = δ ($^{15}NH_4Cl$, solid) − 341.168 ppm was used to convert the ^{15}N chemical shifts from the nitromethane scale to the solid external $^{15}NH_4Cl$ scale.[56] We note that often spectra are referenced to the

dx.doi.org/10.1021/ja408988z | J. Am. Chem. Soc. 2013, 135, 18160−18175

Table 1. ^{13}C and ^{15}N Chemical Shifts of PLP Aldimines in Enzymes and Poly-L-lysine

						δ ^{13}C/ppm			δ ^{15}N/ppm		
figure	PLP	amine	aldimine	tag	environment	C-4′	C-5′	CO-PLL	N-4′ **1s-e**/**1s-k**	NH_2/NH_3^+	N-1
1a	^{15}N-PLP	*p*-toluidine	*N*-(pyridoxylidene)-tolylamine	**2**	freon[a]						277.44 ± 0.05
1b	^{15}N-PLP	methyl amine	*N*-(pyridoxylidene)-methylamine	**3**	H_2O pH 7.6						262.53 ± 0.05
1c	^{15}N-PLP	Lys39 of AlaR	holoenzyme alanine racemase		lyophilized						272
1d	^{15}N-PLP	Lys39 of AlaR	holoenzyme alanine racemase		frozen water						262
2a	^{15}N-PLP	*p*-toluidine	1:1 complex *N*-(pyridoxylidene)-tolylamine with AH	**2**	Freon[a]						237.70 ± 0.05
2a	^{15}N-PLP	*p*-toluidine	1:2 complex *N*-(pyridoxylidene)-tolylamine with AH	**2**	Freon[a]						180.79 ± 0.05
2b	^{15}N-PLP	Lys285 of AspAT	maleate-liganded AspAT		microcryst. with maleate						180 ± 8.0
2c	^{15}N-PLP	Lys285 of AspAT	holoenzyme AspAT		microcryst.						174 ± 8.0
2d	^{15}N-PLP	Lys285 of AspAT	holoenzyme AspAT		10% D_2O						167.4 ± 0.6
4e	^{15}N-PLP	PLL	1:1 PLP/PLL aldimine lyoph. pH 9	**1s**^{P}	dry + HCl						174
3d	^{15}N-PLP	PLL	1:1 PLP/PLL aldimine lyoph. pH 9	**1s**^{P}	dry						270
3c	PLP	^{15}N-ε-PLL	1:1 PLP/PLL aldimine lyoph. pH 12	**1s**′	dry				281	−13	
3a	$^{13}C_2$-4′,5′-PLP	^{15}N-ε-PLL	1:2 PLP/PLL aldimine	**1s**″	dry	161	61		276	−9/−21	
3b	$^{13}C_2$-4′,5′-PLP	^{15}N-ε-PLL	1:1 PLP/PLL aldimine lyoph. pH 9	**1s**″	dry	196/161	61		276		
4b	$^{13}C_2$-4′,5′-PLP	^{15}N-ε-PLL	1:1 PLP/PLL aldimine lyoph. pH 9	**1s**″	5 H_2O per aldimine	161	61		269	−9.2/−21	
4c	$^{13}C_2$-4′,5′-PLP	^{15}N-ε-PLL	1:1 PLP/PLL aldimine lyoph. pH 9	**1s**″	21 H_2O	196/161	61		243		
4d	$^{13}C_2$-4′,5′-PLP	^{15}N-ε-PLL	1:1 PLP/PLL aldimine lyoph. pH 9	**1s**″	dry + HCl	196/161	61		160−190	0	
4f	$^{13}C_2$-4′,5′-PLP	^{15}N-ε-PLL	1:1 PLP/PLL aldimine lyoph. pH 9	**1s**″	4 H_2O per aldimine + HCl	186/80	61			−4	
5	$^{13}C_2$-4′,5′-PLP	^{15}N-aspartic acid + PLL	1:1:1 PLP/PLL/aspartic acid lyoph. pH 9	**1s**′	dry	162	61		273/147	1.1/−4.4	

[a]Mixture of CDF_3/CDF_2Cl.[60]

dx.doi.org/10.1021/ja408988z | J. Am. Chem. Soc. 2013, 135, 18160−18175

liquid ammonia scale, where $\delta(NH_3, liq.) \approx \delta$ ($^{15}NH_4Cl$, solid) + 40.7 ppm.[57] The external standard for ^{13}C spectra was TSP.[56,57]

The ^{13}C and ^{15}N spectra of the solid enzymes and of the aldimines embedded in poly-L-lysine were measured on a Varian Infinity Plus (14 T) solid-state NMR spectrometer (599.9 MHz for ^1H, 150.9 MHz for ^{13}C, and 60.8 MHz for ^{15}N) with a 4 mm HX probe. Solid-state NMR spectra of Figure 4b–d,f were recorded with a Varian Infinity Plus (7 T) NMR spectrometer (300.1 MHz for ^1H, 75.5 MHz for ^{13}C, and 30.4 MHz for ^{15}N) with a 6 mm HX probe. Standard ramp cross-polarization CP NMR experiments were performed under magic angle spinning (MAS) conditions. The NMR pulse and acquisition parameters are listed in Table S1 of the Supporting Information. The chemical shifts of the different samples and their assignment are assembled in Table 1.

H-Bond Correlations. The H-bond correlations used to estimate H-bond geometries from ^1H and ^{15}N chemical shifts of OHN H-bonds have been described previously for pyridine–acid complexes[58] and for PLP and its acid complexes.[37,38,59]

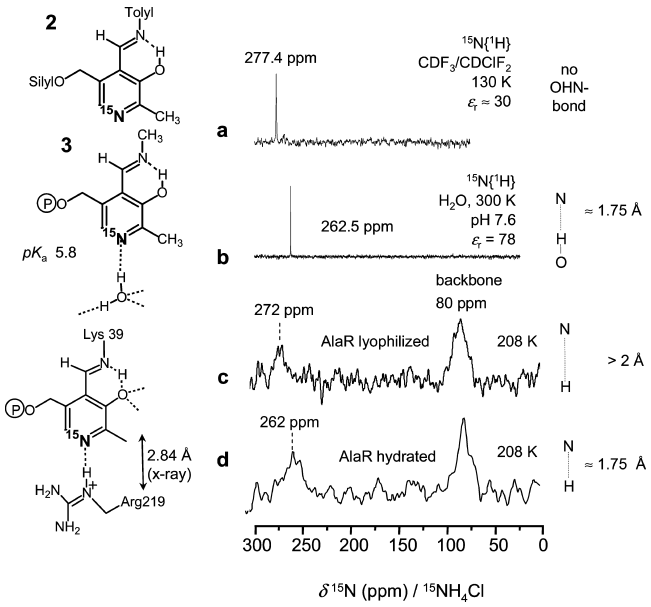

Figure 1. ^{15}N NMR spectra of ^{15}N-PLP aldimines under various conditions. (a) Aldimine **2** at 11.7 T at 130 K in CDF_3/CDF_2Cl. Adapted from ref 39. (b) Aldimine **3** at 11.7 T in an aqueous solution at pH 7.6, adapted from ref 34. (c) Solid-state CPMAS spectra at 14 T and a spinning speed of 8 kHz of dry enriched alanine racemase lyophilized from frozen propanol/dry ice. (d) Same as for part c, but after hydration to a water content of about 36%.

RESULTS

^{15}N NMR of ^{15}N-PLP in Alanine Racemase (AlaR). In Figure 1, we present ^{15}N spectra of ^{15}N-PLP in AlaR and of ^{15}N-PLP model systems under various conditions. Figure 1a shows a spectrum of a model system, *p*-tolyl aldenamine **2**, dissolved in polar aprotic Freon mixture CDF_3/CDF_2Cl, where the pyridine ring is not involved in hydrogen bonding or only in a very weak hydrogen bond with the solvent. Therefore, the spectrum was taken at 130 K where the solvent exhibits a dielectric constant of 30.[60] For solubility reasons, the 5-′OH groups were silylated.

The chemical shift of 277 ppm is typical of the free base.[58] By contrast, in the case of an aqueous solution, methylamine aldimine **3** exhibits at pH 7.6 a chemical shift of 262.5 ppm as shown in Figure 1b. Under these conditions, the pyridine nitrogen is H-bonded to water molecules. Using chemical shift correlations described previously,[36−39] we estimate an average N···H distance of 1.75 Å.

In Figure 1c, we present the ^{15}N CPMAS NMR spectrum of dry lyophilized AlaR where the pyridine nitrogen was labeled with ^{15}N. The spectrum was measured at 208 K in order to improve the spectral resolution by reducing molecular motions. A signal at 272 ppm exhibiting a line width of about 15 ppm is observed for the ^{15}N-labeled cofactor along with a broad backbone signal at around 80 ppm. A control spectrum with lyophilized AlaR containing nonlabeled PLP was taken, which confirms the chemical shift of the peptidic backbone at 78 ppm. For the case of a lyophilized sample, these signals are surprisingly sharp.[57] The position and width of the ^{15}N signal indicate a broad distribution of N···H distances characterized by an average distance of at least 2 Å, typical of a very weak hydrogen bond.

When we hydrated the lyophilized AlaR sample to a water content of about 36% and remeasured the sample at 208 K where water is frozen, we observed a high-field shift to 262 ppm (Figure 1d). This value indicates a shortening of the average N···H distance to a value of about 1.7 to 1.8 Å as found for **3** in water. We interpret these findings later in the Discussion.

^{15}N NMR of ^{15}N-PLP in AspAT. In Figure 2, ^{15}N spectra of ^{15}N-PLP in AspAT and of model system **2** dissolved in polar mixture CDF_3/CDF_2Cl are depicted. Figure 2a shows a spectrum obtained after adding acid Boc-Asp-OtBu to **2**, which models the Asp222–pyridine hydrogen bond illustrated in Scheme 2a. In agreement with previous studies of pyridine–acid complexes,[58,61] the formation of a 1:1 complex with the acid is observed at 238 ppm, corresponding to an H···N distance of 1.43 Å. A 2:1 complex is also observed, which resonates at 181 ppm. Thus, a zwitterionic structure with a pyridine H···N distance of 1.1 Å results, which reflects the increased acidity of the aspartic acid dimer compared to that of the monomer.

Figure 2b,c depict the solid-state ^{15}N CPMAS NMR spectra of microcrystalline holo-AspAT in a closed conformation that is ligand bound to inhibitor maleate and unbound in an open conformation, both containing ^{15}N in the pyridine ring of PLP. The ^{15}N signals resonate at 175 and 180 ppm, whereas the signals of the nitrogen atoms of the AspAT backbone appear at around 80 ppm. Using the ^{15}N chemical shift-distance correlation for PLP models,[37−39] we estimate average N–H distances of 1.11 and 1.09 Å, where the corresponding H···O distances are 1.49 and 1.54 Å. These results clearly indicate a zwitterionic structure for the intermolecular OHN hydrogen bond in AspAT. The sum of the N···H and H···O distances, 2.60 and 2.63 Å for the AspAT species depicted in Figure 2b,c are in excellent agreement with those of 2.58 and 2.64 Å obtained by X-ray crystallography.[40b]

Finally, we dissolved AspAT in water at pH 7.5 and obtained the ^{15}N spectrum presented in Figure 2d. A slight high-field shift to 167.4 ppm was observed, as well as an extreme narrowing of the signal. The latter indicates a high local molecular mobility, whereas the former is in agreement with a slight shortening of the NH-bond to 1.07 Å and a lengthening of the O···H distance to 1.64 Å. This corresponds to an increase in the local dipole moment, as expected from an increase in the

dx.doi.org/10.1021/ja408988z | J. Am. Chem. Soc. 2013, 135, 18160−18175

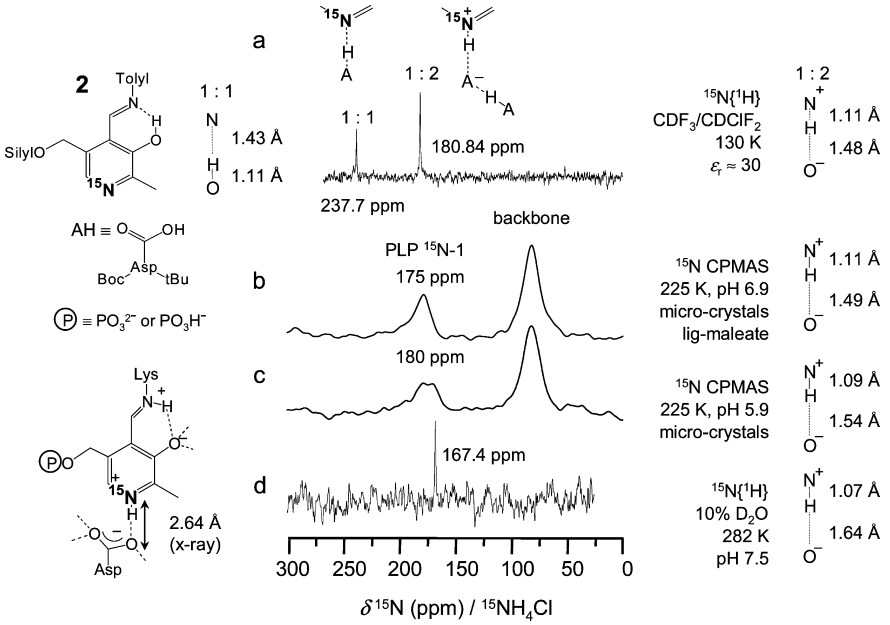

Figure 2. ^{15}N NMR spectra of ^{15}N-PLP aldimines under various conditions. (a) 90° single-pulse spectra of **2** in CDF_3/CDF_2Cl at 11.7 T and 130 K after the addition of a protected aspartic acid. Solid-state CPMAS spectra at 14 T and a spinning speed of 7 kHz of (b) dry microcrystalline maleate-liganded holo-AspAT and (c) microcrystalline holo-AspAT. (d) 90° single-pulse spectra of holo-AspAT in aqueous solution. Adapted from ref 42.

local dielectric constant. The implications of these findings are discussed below.

Solid-State ^{13}C and ^{15}N CPMAS NMR of PLP in Poly-L-lysine. In this section, we describe the ^{13}C and ^{15}N NMR spectra of PLP-forming aldimines **1s** with poly-L-lysine (PLL), mostly obtained under CPMAS conditions. The different isotopically labeled PLP and PLL species employed are presented in Scheme 4 and are labeled accordingly with superscripts or subscripts. As described in the Experimental Section, the samples were prepared by mixing both components in aqueous solution at a given pH and subsequent lyophilization. Residual water was removed in vacuo. The formation of aldimines depends on pH. ^{15}N CPMAS spectra of **1s^{p}** indicate that formation is maximal at around pH 9 as presented in Figure S1 of the Supporting Information. Therefore, we prepared most samples at pH 9 but some of them also at higher pH. We observed that the change in the molecular weight of PLL did not lead to noticeable changes in the ^{13}C and ^{15}N spectra and hence the H-bond and protonation states of the PLP aldimines. Therefore, we did not repeat experiments carried out using the low molecular weight PLL_l and worked later with the high molecular weight PLL_h.

Scheme 4. ^{13}C and or ^{15}N Isotopically Enriched Species Investigated in This Study[a]

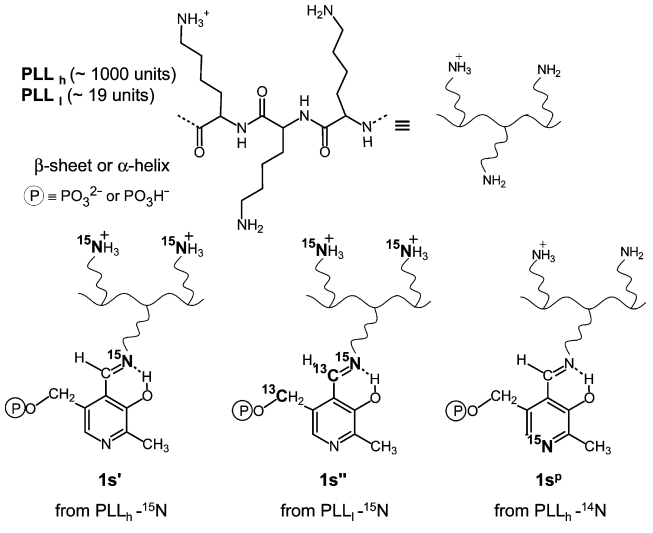

[a]The free ε-amino groups are shown partially protonated because the pH value was set close to the pK_a value of poly-L-lysine (pK_a = 9.85[51a]).

Dry Samples. Figure 3a shows the ^{13}C and ^{15}N CPMAS NMR spectra of dry **1s″** in a sample obtained by mixing $^{13}C_2$-4′,5′-PLP and $^{15}N_\varepsilon$-PLL in a ratio of 1:2. Asterisks are used to label rotational side bands. The aldimine ^{13}C-4′ signal appears at 160 ppm, and the ^{13}C-5′ signal appears at 61 ppm as expected from previous studies of aldimine models in aqueous solution.[6] No signal is observed for free PLP **1a** or for gem-diamine **1g**. According to our previous studies of a model gem-diamine of PLP with diaminopropane, **1g** should contribute a ^{15}N-4′ peak at 10 ppm to the ^{15}N spectrum and a ^{13}C-4′ peak at 70 ppm to the ^{13}C spectrum.[6] The corresponding ^{15}N signal of **1s″** appears at 275 ppm. A broad, somewhat structured signal is observed at high field for residual amino groups; this signal is smaller than expected for a 1:2 ratio of PLP and the lysine residues of PLL. Although spin dynamics in the CPMAS experiment affect the signal intensities, we think that the lyophilized sample contained more PLP than the 1:2 ratio of the solution before lyophilization. Our experience throughout this study was that the final sample composition might be different from the expected one. The sample compositions indicated are then nominal uncorrected numbers.

When we increased the amount of PLP to form 1:1 samples, we observed similar spectra, but now free PLP aldehyde signal **1a** was observed at around 200 ppm (Figure 3b). No amino group signal could be detected in the ^{15}N CPMAS spectrum. Thus, there appears to be a slight excess of PLP in the sample.

dx.doi.org/10.1021/ja408988z | J. Am. Chem. Soc. 2013, 135, 18160−18175

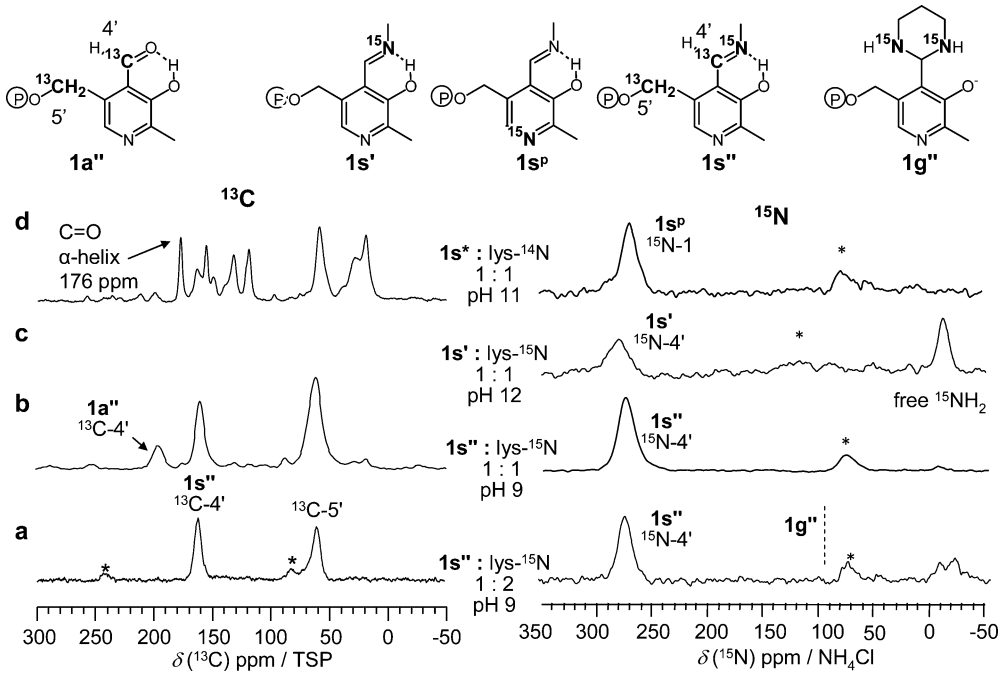

Figure 3. (a) ^{13}C and ^{15}N CPMAS spectra of a 1:2 mixture of $^{13}C_2$- 4′,5′-PLP in ^{15}N-PLL$_h$ lyophilized from aqueous solutions at pH 9 and recorded at room temperature at 14 T. The vertical dashed line indicates the ^{15}N chemical shift expected for **1g**″.[6] (b) ^{13}C and ^{15}N CPMAS spectra of a 1:1 mixture of $^{13}C_2$- 4′,5′-PLP in ^{15}N-PLL$_l$ lyophilized from aqueous solutions at pH 9 and recorded at 14 T. (c) ^{15}N CPMAS spectra of a 1:1 mixture of PLP in ^{15}N-PLL$_h$ lyophilized from aqueous solutions at pH 12 recorded at 14 T. (d) ^{13}C and ^{15}N CPMAS spectra of a 1:1 mixture of ^{15}N-PLP in PLL$_h$ lyophilized from aqueous solutions at pH 11. The samples were spun at the magic angle at a rate of 6 kHz for the ^{13}C spectra and at 7 kHz for the ^{15}N spectra. All measurements were performed at room temperature.

For comparison, we have presented in Figure 3c a ^{15}N CPMAS spectrum of **1s**′ lyophilized at pH 12. A small low-field shift to 280 ppm that is compatible with the deprotonation of the phenolic OH group is observed.[6] Now, a strong signal for the free amino groups is observed at −15 ppm, as expected from previous studies of PLL.[51] The appearance of this signal illustrates that the equilibrium constant for the formation of the aldimine species is reduced at high pH.

To determine the protonation state of the pyridine nitrogen, we measured a sample containing ^{15}N-PLP with unlabeled PLL. The result is presented in Figure 3d. Species **1s^{P}** contributes a signal to the ^{15}N spectrum at 271 ppm, which is the same value found for AlaR (Figure 1c). It indicates that the pyridine nitrogen is free or involved only in a very weak H-bond. In the corresponding ^{13}C spectrum, carbons of both **1s^{P}** and PLL contribute. The signals of the latter have been described previously.[51,62] We did not try to assign all signals in this study because it was beyond the scope. However, the finding of a sharp ^{13}C signal for the carbonyl group of PLL at 176 ppm is important. This value is diagnostic of an α-helical conformation of PLL,[60] whereas β-pleated sheets contribute a broader signal at 172 ppm. In principle, the signals of the α-CH carbons of the polypeptide backbone are also of diagnostic value for the PLL conformation but overlap here with the C-5′ signal.

Hydrated and Acidified Samples. To facilitate the interpretation of our results with AlaR and AspAT, we hydrated samples, exposed dry samples to HCl gas, and hydrated samples previously exposed to HCl gas. The results are presented in Figure 4.

For comparison, we show again in Figure 4a the spectra of the 1:2 sample from Figure 3a. Hydration with ∼5 water molecules per PLP leads to a small high-field shift of the ^{15}N-4′ signal of **1s**″ as illustrated in Figure 4b. The amino group signal appears at around 0 ppm, split into two parts. The high-field part exhibits a chemical shift typical of free $^{15}NH_2$ groups, and the low-field part exhibits a chemical shift typical of hydrated $^{15}NH_2$ groups as previous hydration studies of PLL have shown.[51c] The ^{13}C spectra are unchanged and still exhibit the chemical shifts typical of the ^{13}C-4′ and the ^{13}C-5′ positions of **1s**″.

When part of the dry 1:1 sample of Figure 3b was hydrated with ∼21 water molecules per PLP−PLL aldimine, we obtained the spectra presented in Figure 4c. Again, the ^{13}C spectra exhibit few changes; in particular, a small amount of free PLP persists. However, the ^{15}N-4′ signal of **1s**″ is shifted to high field and is substantially broadened. No free amino groups are detectable in this sample, in view of the excess **1a**″. The addition of water does not interconvert **1a**″ and **1s**″ rapidly on the NMR time scale. Thus, the broadening of the ^{15}N-4′ signal of **1s**″ cannot arise from the hydrolysis of **1s**″. The Gaussian line shape indicates that the broadening of ^{15}N-4′ is inhomogeneous, arising from a distribution of chemical shifts. The shift of the signal to high field can be explained in terms of the fast tautomerism between enolimine tautomer **1s-e** and ketoenamine tautomer **1s-k** presented in Scheme 1, induced by the addition of water. A quantitative analysis of the high-field shift will be presented later.

Part of the dry 1:1 sample of Figure 3b was exposed to HCl gas at 1 atm for 10 min in a desiccator. The resulting sample gave the ^{15}N CPMAS spectrum presented in Figure 4d. Now, the ^{15}N-4′ signal shifts to higher field. Two components are observed as illustrated in Figure 4d: a broad one at 180 ppm and a sharper one at 160 ppm. This indicates that ketoenamine form **1s-k** dominates. A broad amino signal is observed, exhibiting superposed broad and sharper components at around 0 ppm.

dx.doi.org/10.1021/ja408988z | J. Am. Chem. Soc. 2013, 135, 18160−18175

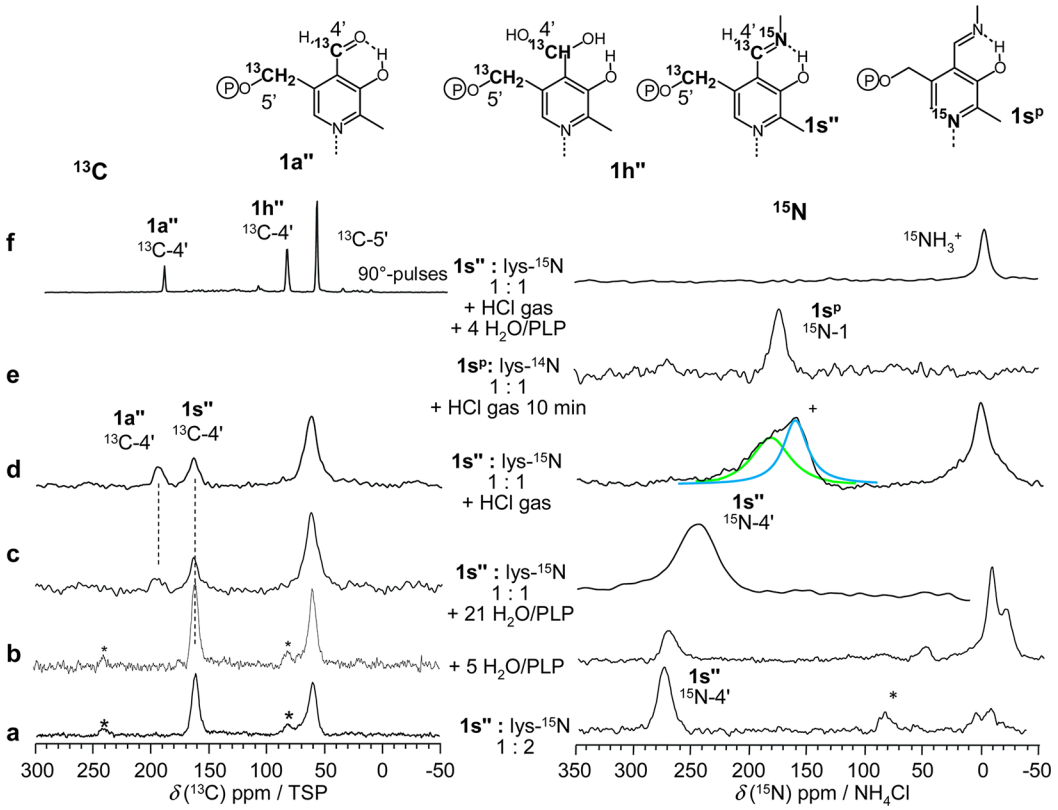

Figure 4. ^{13}C and ^{15}N CPMAS NMR spectra of lyophilized samples of poly-L-lysine (PLL) containing pyridoxal 5′-phosphate under various conditions: (a) at 14 T for a 1:2 mixture $^{13}C_2$-4′,5′-PLP + ^{15}N-PLL$_l$; (b) at 7 T for a 1:1 mixture $^{13}C_2$-4′,5′-PLP + ^{15}N-PLL$_l$ hydrated with 5 water molecules per aldimine; (c) the same as in b but hydrated with 21 water molecules per aldimine; (d) the same as in b but instead of being hydrated the sample was exposed to gaseous HCl for 10 min; (e) at 14 T for a 1:1 mixture of ^{15}N-PLP with PLL$_h$ exposed to gaseous HCl for 10 min; (f) the same sample as in b but obtained by 90° pulses after hydration with 4 water molecules per aldimine and then exposed to gaseous HCl for 10 min. All measurements were performed at room temperature. The sample was spun at the magic angle at a rate of 6 kHz for the ^{13}C spectra and at 7 kHz for the ^{15}N spectra.

We repeated the experiments with the sample in Figure 3d containing ^{15}N-pyridine-labeled **1s^p** in order to probe how the pyridine nitrogen responds to HCl gas. As depicted in Figure 4e, the ^{15}N signal of this sample is also shifted to high field by HCl addition and appears at 190 ppm. However, hydrolysis takes place immediately after exposure of the acidified samples to water vapor: the addition of ∼4 water molecules per aldimine unit is sufficient for hydrolysis to occur in the solid state. This is illustrated in Figure 4f. In the ^{15}N spectrum, only the signal of the protonated amino group is observed at about −2 ppm. This value is typical of α-helical $NH_3^+Cl^-$ salt bridges hydrated by a small number of water molecules.[51c] In the ^{13}C spectrum, the aldimine carbon signal has disappeared and PLP is present only as aldehyde **1a** and as hydrate **1h**, exhibiting their well-known chemical shifts.[6,35] The intensity ratio of both signals is typical of an aqueous solution of pH 4.

Solid-State ^{13}C and ^{15}N CPMAS NMR of PLP−PLL in the Presence of Aspartic Acid. To obtain preliminary information about the protonation states of external aldimines, we lyophilized an aqueous solution of unlabeled PLL at pH 9 with 1 eq. of doubly ^{13}C-labeled **1a**″ and 1 eq. of ^{15}N-labeled aspartic acid per lysine residue. The ^{13}C and ^{15}N CPMAS spectra are presented in Figure 5.

Now, both the amino groups of PLL and those of the aspartic acid residues compete for the PLP. As a consequence, no free PLP is observable in the ^{13}C spectrum; only the aldimine signals that stem from both the PLL and aspartic acid aldimines are seen.

By contrast, the ^{15}N signals originate only from aspartic acid, which experiences different environments. A "free" amino group signal is observed at high field, with two components at −1.4 and −4.4 ppm. The formation of the aspartic acid aldimine leads to two broad ^{15}N-4′ signals, one at 275 and the other at 147 ppm. Clearly, the low-field signal stems from enolimine tautomer **1s**″**-e** and the high-field signal from the ketoenamine tautomer **1s**″**-k** (Scheme 1). It is remarkable that the two signals are in slow exchange. Therefore, because proton transfer between the two tautomers is usually very fast, the two tautomers are located in different environments, which dictate the tautomeric state.

At higher fields, the free amino group signal and the two aldimine signals exhibit comparable intensities. Therefore, about half of the aspartic acid forms an aldimine, and the other half is free. Because there is no free PLP in the sample, the amount of internal aldimine formed is similar to that of external aldimine. A similar result was obtained for an aqueous solution where PLP forms aldimines both with the ε-amino and α-amino groups of free L-lysine.[6] We will interpret these findings later in the Discussion.

Determination of Equilibrium Constants of Tautomerism. The ^{15}N-4′ signals of the spectra presented above provide information about the equilibrium constants K_t of tautomerism,

dx.doi.org/10.1021/ja408988z | J. Am. Chem. Soc. 2013, 135, 18160−18175

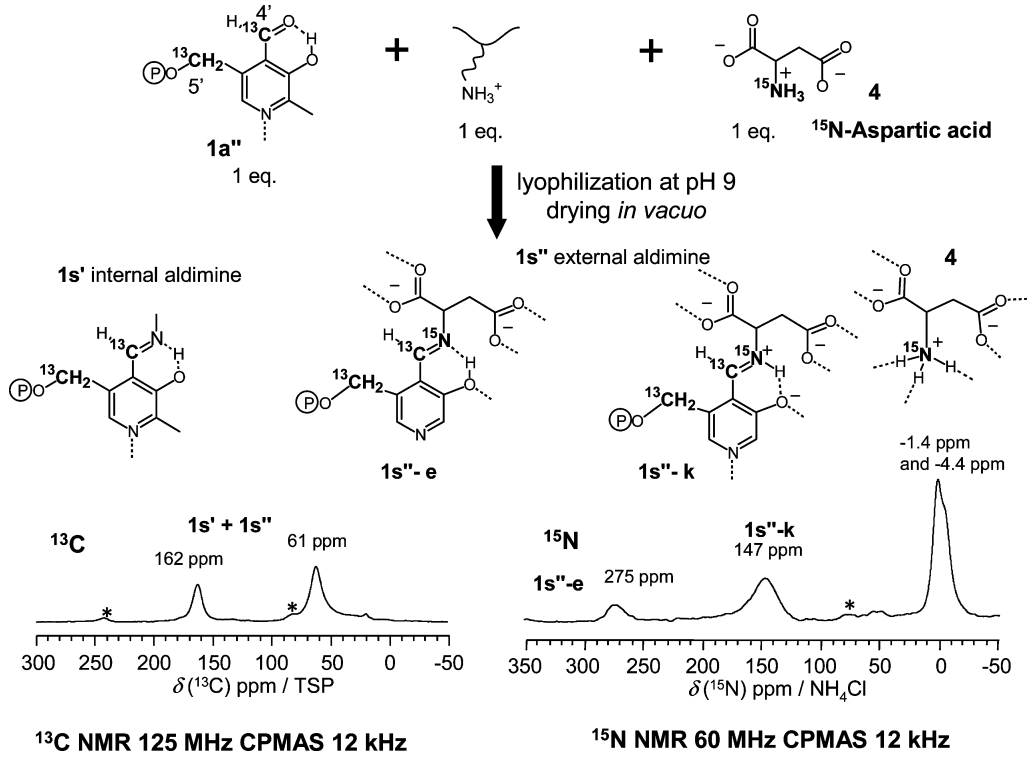

Figure 5. ^{13}C and ^{15}N CP MAS NMR spectra at 14 T, room temperature, and spinning rates of 6 and 7 kHz, respectively, for a 1:1:1 mixture of $^{13}C_2$-4′,5′-PLP, PLL_l, and ^{15}N-aspartic acid lyophilized at pH 9.

which is a fast process. The average ^{15}N-4′ chemical shift is given by

$$\delta = x_e\delta_e + x_k\delta_k = \frac{\delta_e + K_t\delta_k}{1 + K_t} \quad (7)$$

where x_e and x_k represent the mole fractions of the enolimine and the ketoenamine forms, δ_e and δ_k represent the corresponding limiting chemical shifts, and K_t represents the equilibrium constant of tautomerism. In principle, δ_e and δ_k can vary with K_t,[38] but we will neglect this dependence here. Equation 7 can be recast in the form

$$K_t = \frac{x_k}{x_e} = \frac{\delta - \delta_e}{\delta_k - \delta} \quad (8)$$

Equation 8 is useful for deriving K_t from the average chemical shifts δ observed. Because the calculated values depend on the values of the limiting chemical shifts, their choice is very important. These shifts cannot be directly observed for the systems studied and need, therefore, to be estimated from model systems.

The value of δ_e is most easily obtained from the spectra in Figure 3a,b, which indicate a value of 275 ppm. The same value is also obtained from the low-field ^{15}N signal in Figure 5. This indicates that the value does not differ much between the external and the internal aldimine. We note that it would not be correct to use the slightly larger value for the deprotonated negatively charged species of Figure 3c. The value of δ_k needs to be taken from a Schiff base model where it is clear that only the ketoenamine form is present. Previously, for aqueous solutions, values of about 140 ppm were observed for this form.[6] The same value was also observed for a solid complex of the methylamine aldimine with strong organic acids.[37] Using both values, we calculated the equilibrium constants listed in Table 2.

Table 2. ^{15}N Chemical Shifts δ_k and Calculated Equilibrium Constants, K_t, of the Enolimine-Ketoamine Tautomerism of PLP Aldimines in Poly-L-lysine and Enzyme Environments

system	ref	δ_k/ppm	K_t
1s″+ 4 H_2O	here	270	0.04
1s″+ 21 H_2O	here	245	0.3
1s″+ HCl	here	180	2.4
1s″+ HCl	here	160	5.8
1s″+ aspartic acid	here	147	∼20
external aldimine of AlaR with (1-aminoethyl) phosphonic acid	49	150	13
external aldimine of tryptophan synthase with aminoacrylate and indole	50	257.2	0.15

DISCUSSION

We have studied the H-bonding and proton tautomerism of isotopically labeled pyridoxal 5′-phosphate as an internal aldimine in AlaR, AspAT, and PLL using ^{13}C and ^{15}N solid-state NMR. In addition, we studied an external aldimine with aspartic acid in PLL. In this section, we discuss these findings and their implication for enzymatic reaction mechanisms.

Intermolecular OHN H-Bond of Internal Aldimines of PLP in AspAT and AlaR: Effect of Hydration. Using the ^{15}N H-bond correlations described previously for H-bonded pyridines,[58] adapted for PLP,[39] we have shown by comparison with model systems (Figure 3) that the pyridine nitrogen is protonated in microcrystalline AspAT. We estimate an O···H distance of 1.54 Å and an H···N distance of 1.09 Å. The sum of these distances (2.63 Å) is identical to the value of 2.64 Å

dx.doi.org/10.1021/ja408988z | J. Am. Chem. Soc. 2013, 135, 18160−18175

found by X-ray crystallography.[40b] When AspAT is dissolved in aqueous solution, the OHN bonding interaction is maintained; the HN distance is slightly shortened and the O···H distance is slightly lengthened, as expected for an increase in the local polarity. The formation of H-bonds to water is not compatible with these findings (Figure 2d). In other words, in the case of AspAT, the H-bond structure of the solid-state (Scheme 2) is maintained in aqueous solution (i.e., the pyridine−aspartate H-bond is maintained in a nonaqueous environment).

By contrast, the ^{15}N chemical shifts of AlaR (Figure 1) indicate the following. The pyridine ring of the dry lyophilized solid is not protonated and is involved only in a very weak hydrogen bond, most probably to Arg224. The estimated N···H distance is 2 Å or longer. This value is not compatible with the value of about 1.8 Å that we estimate from the crystallographic N···N distance of 2.84 Å (Scheme 2) assuming an arginine NH distance of 1 Å.

However, the pyridine N···H distance shortens to the expected crystallographic value upon hydration of the lyophilized solid (Figure 1). Initially, we considered that the pyridine−arginine NHN H-bond might be broken and replaced by a pyridine−water NHO H-bond. However, this would weaken the PLP−enzyme interaction considerably and allow the PLP cofactor to enter the bulk aqueous solution easily, in contrast to the experimental findings. Thus, in aqueous solution, ^{15}N-PLP can enter only the apoenzyme but does not exchange with the unlabeled cofactor. We also note that Major et al.[48] included water in their calculations but did not see the arginine−pyridine H-bond being broken. Also, the crystal structures are determined in crystals that contain ∼50% water where the Arg219−pyridine interaction is stable.

Therefore, we propose that upon hydration lyophilized AlaR adopts a structure typical of the crystalline state. This can be rationalized in terms of the absence of the two water molecules near PLP (Scheme 2b) in the lyophilized dry state but by their presence in the hydrated state.

These findings prove that the pyridine ring of AlaR is not protonated, as suggested by X-ray crystallographic results, and that it is necessary to look for an alternate means of PLP activation other than N-protonation.

PLP in PLL as a Model Protein Environment. We used solid lyophilized PLL (Scheme 4) as a model environment in order to obtain information about the intramolecular H-bond of PLP aldimines that is difficult to obtain directly. The advantages of PLL are (i) that internal and external PLP aldimines are easily formed, (ii) that the water content can be controlled, (iii) that the samples can be lyophilized at different pH values or the acid contents can be controlled by exposure to gaseous acids or bases, and (iv) that the amino groups of the side chains can be relatively easily labeled with ^{15}N.

PLL is a polypeptide that can adopt a β-pleated sheet or an α-helical conformation. β-Pleated sheets are formed only from salts with halogen acids.[51] On hydration, the NHX H-bonds are replaced by NHO H-bonds with water because space between sheets is limited. Therefore, we did not expect the formation of the β-pleated sheet conformation when most lysine amino groups form an internal aldimine with PLP because of its large size. Indeed, the lyophilization of solutions of PLL in the presence of PLP at pH 9 leads to aldimines (**1s**) of PLP, whose structures are discussed below. By ^{13}C NMR, we observe a peak for the CO groups of PLL that is typical of a purely α-helical conformation of PLL[51,60] (Figure 3d), as expected. As shown in the following section, we were able to reproduce the known ^{15}N chemical shifts of PLP aldimines in enzymes using PLL as a model environment.

Structure of the PLP−PLL Aldimine in the Absence of Water and Acids. To obtain more information about the coupling of the intermolecular H-bond to the pyridine nitrogen with the intramolecular OHN H-bond of the aldimine, we performed ^{13}C and ^{15}N solid-state NMR studies on the aldimines of PLP in PLL. Either the pyridine nitrogen was labeled with ^{15}N but not the lysine side chain amino groups or PLP was doubly labeled with ^{13}C and the side chains of PLL were labeled with ^{15}N. In previous studies, we characterized the interactions of the amino groups of PLL with acids and water.[51]

As shown in Figure 3, by ^{13}C NMR, we could easily detect the formation of PLP aldimines **1s** as well as the presence of unreacted PLP as aldehyde **1a** or hydrate **1h** (Scheme 1). The equilibrium constant for aldimine formation in water is maximized at pH 9, the pH value used here. When PLL labeled with ^{15}N in the side chains is used, the aldimine nitrogen in the 4′ position is labeled with ^{15}N and provides information about the state of the intramolecular OHN H-bond.

After lyophilization at pH 9, a comparison of the ^{15}N chemical shift of 272 ppm of the aldimine nitrogen (Figure 3a,b) with values obtained previously for model solids[36] and solutions[39] indicates that only enolimine form **1s-e** (Scheme 1) is present. Also, the value of the ^{15}N chemical shift of 275 ppm for the pyridine nitrogen indicates that it is not protonated and that it forms either no bond or a weak H-bond (Figure 3d). This value is the same as that found for AlaR (Figure 1c), indicating that in the absence of water and acid PLL reproduces the H-bond and protonation state of the pyridine nitrogen in AlaR.

Absence of Gem-Diamine Formation. With PLL as a model environment, we expected to observe gem-diamine species **1g** (Scheme 1) when the amino groups are present in excess (e.g., the PLP/PLL 1:2 samples) or at higher pH. However, the peaks expected from previous model studies[6] are not observed. This may be the result of several factors. First, even in aqueous solution PLP-L-lysine aldimines do not form gem-diamines if an excess of L-lysine is present. This means that the gem-diamines are unfavored energetically. Second, in α-helical PLL the amino side chains point in different directions, which means that the formation of a gem-diamine between amino groups of adjacent residues is less likely.

Protonation of PLP Aldimine in PLL and H-Bond Coupling. In previous studies, we found that, in the case of model PLP−methylamine aldimine complexes with carboxylic acids in polar solution, the inter- and intramolecular OHN H-bonds are coupled.[39] That is, when the H of the OHN H-bond with a carboxylic acid is located on the pyridine nitrogen, a shift of the H in the intramolecular OHN H-bond occurs toward the aldimine nitrogen. Because the ^{15}N chemical shifts of both H-bonds are a function of the average proton positions, these shifts can be used to detect the H-bond coupling.

For that purpose, we exposed PLP−PLL samples lyophilized at pH 11 to gaseous HCl for 10 min. The resulting ^{15}N CPMAS spectra (Figure 4d,e) indicate that both the pyridine and the aldimine nitrogen signals are shifted by ∼100 ppm to high field as a result of the protonation of the pyridine nitrogen and the ensuing dominance of the ketoenamine form as a result of H-bond coupling. As discussed previously,[39] this behavior was also observed for aliphatic aldimines in highly polar local environments. The chemical shift of the pyridine nitrogen (172 ppm)

is close to that in AspAT (Figure 2b,c). This indicates again that PLL is a good model protein environment for examining PLP protonation states.

The chemical shift of 160 to 180 ppm for the aldimine nitrogen (Figure 4d) indicates that ketoenamine form **1s-k** is not completely formed, for which a value of 140 ppm is expected.[36] However, the signal is broad and consists of two unresolved features, indicating two slightly different environments, with each exhibiting a distribution of equilibrium constants of the enolimine−ketoenamine tautomerism. In other words, the equilibrium constants and hence the ^{15}N signal positions depend on the local environment, which varies with the inhomogeneity of the sample. Environmental differences could arise from different numbers of water molecules or other structural inhomogeneities. Similar distributions of equilibrium constants of tautomerism have been observed and described previously for other inhomogeneous solid polymeric environments.[63]

The question of which species are formed arises, in particular, whether one or two HCl molecules interact with PLP in PLL. Two different structures are proposed in Scheme 5. Previous studies of aldimine models show that when a strong proton donor forms a strong H-bond to the phenolic oxygen (or protonates the latter) the equilibrium constant greatly favors ketoenamine formation.[64] This means that the two signal components at 180 ppm are compatible with a 1:1 complex of aldimine with HCl and those at 160 ppm are compatible with a 1:2 complex.

Scheme 5. Possible Structures of PLP Aldimines in Poly-L-lysine Lyophilized at pH 11 after Contact with Gaseous HCl

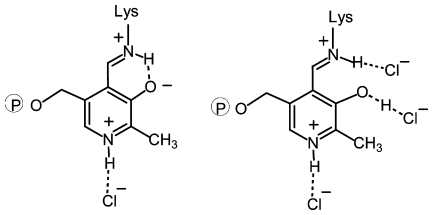

Hydration of PLP Aldimine in PLL. The hydration of a PLP−PLL sample hydrophilized at pH 9 leads to smaller high-field shifts of the aldimine nitrogens compared to the interaction with HCl (Figure 4b,c). The addition of 5 water molecules per PLP in PLL leads to a high-field shift of only 2 ppm, but 21 molecules of water shift the signal to 245 ppm and broaden it considerably. Nevertheless, the introduction of water increases the tautomeric equilibrium constant toward the ketoenamine, as deduced previously[39] and as has been concluded from the computational studies of Gao et al.[48] The equilibrium constants of tautomerism obtained from these shifts are discussed below.

Acid Hydrolysis of the PLP−PLL Aldimine. Alone, neither hydration nor acidification with gaseous HCl led to the hydrolysis of the PLP−PLL aldimine. However, when we added a small number of water molecules to the acidified samples, the aldimine hydrolyzed to PLP aldehyde **1a** and free amino groups of PLL. This finding is noteworthy because it occurred in solid samples under conditions of reduced molecular mobility.

Aldimine Formation of PLP in PLL with Aspartic Acid. To probe the properties of external aldimines, we lyophilized equimolar parts of doubly ^{13}C-labeled PLP **1s″**, ^{15}N-labeled aspartic acid, and unlabeled amino groups of PLL and recorded the ^{13}C and ^{15}N CPMAS spectra depicted in Figure 5. The spectrum contains much information, which is discussed below.

Both the unlabeled amino groups of PLL and the amino group of aspartic acid compete for Schiff base formation with PLP, and no unreacted PLP is observable in the ^{13}C CPMAS spectrum, which is not able to distinguish between internal and external aldimines **1s′** and **1s″**. By contrast, the ^{15}N CPMAS spectrum shows a peak at high field for the amino groups of unreacted aspartic acid and two peaks at 275 and 147 ppm. We assign these peaks to different environments of the external aldimine. The chemical shift of 275 ppm indicates that this environment contains almost the entire enolimine form **1s″-e**, whereas the shift of 147 ppm indicates only the presence of ketoamine form **1s″-k**. In each environment, tautomerism will

Scheme 6. Possible Structures of PLP Aldimines with Aspartic Acid in Poly-L-lysine in the Presence of Excess Aspartic Acid

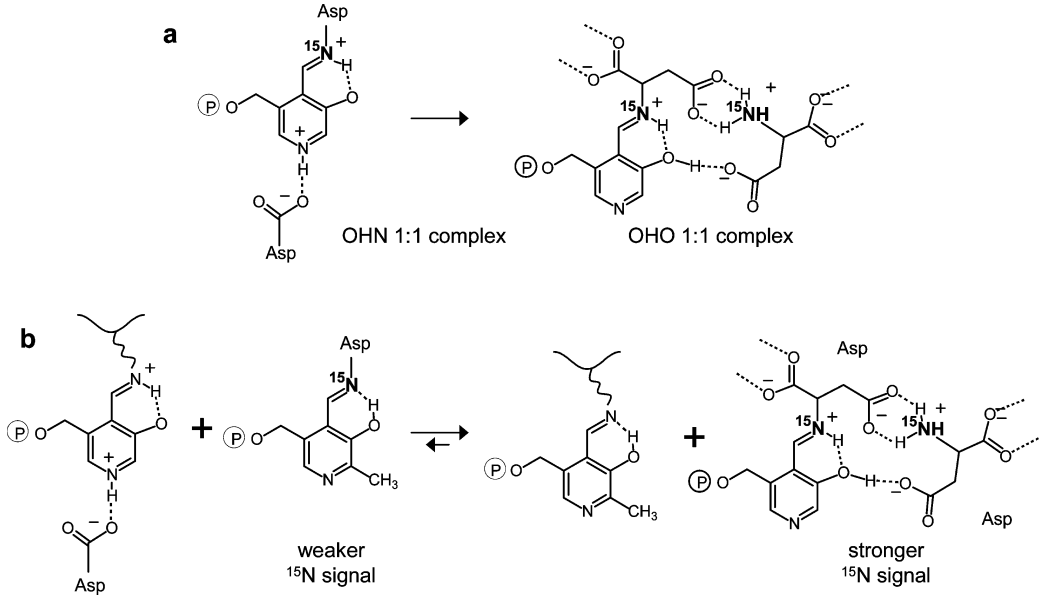

dx.doi.org/10.1021/ja408988z | J. Am. Chem. Soc. 2013, 135, 18160−18175

Scheme 7. Three-Site Tautomerism of a Quinoid Complex of Tryptophan Synthase with Aminoacrylate and Indoline According to Mueller et al.[50]

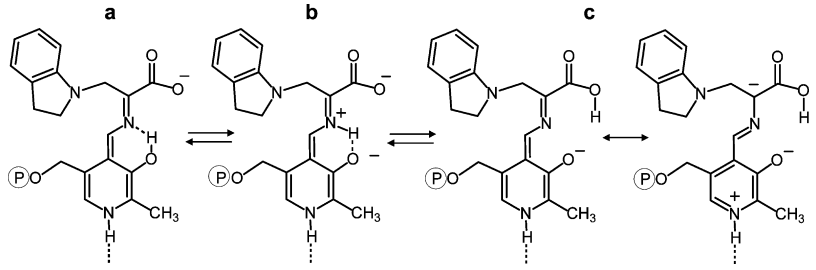

be fast, but the two environments are in slow exchange as discussed below. Although ^{15}N CPMAS is not quantitative, the spectrum indicates that about half of the amino groups of aspartic acid are unreacted whereas the other half are in the external aldimine form. In agreement with the sample composition, this means that internal and external aldimines **1s′** and **1s″** exhibit similar mole fractions. The enolimine peak is much less intense than the ketoamine peak, a feature that is not easy to rationalize at first sight.

The main question that arises is what causes the occurrence and the signal intensity difference of the enolimine and ketoenamine environments. It is evident that in the enolimine environment the pyridine ring is not protonated, in agreement with lyophilization at pH 9, and hence the proton of the intramolecular OHN hydrogen bond is located near the oxygen. By contrast, the interaction of the external aldimine with other unreacted aspartic acid molecules must be the cause of the formation of ketoenamine tautomer **1s″-k**. The simplest possibility is the formation of 1:1 complexes as depicted in Scheme 6. Besides complex formation with the phosphate residue, we need to discuss hydrogen bond interactions of the carboxylic group of an unreacted aspartic acid molecule with either the phenolic oxygen or the pyridine nitrogen. The proton in these hydrogen bonds is taken from the solvent in the last stages of the lyophilization, in a manner similar to pyridine–aspartic acid hydrogen bond formation in AspAT.

We expect a similar hydrogen bond in the absence of a secondary interaction between the two aspartic acid residues as illustrated by the structure of the OHN 1:1 complex in Scheme 6a. However, if a secondary interaction occurs (for example, an interaction of the amino group of the unreacted aspartic acid with the carboxyl group of the aldimine), then it is conceivable that the OHO 1:1 complex depicted in Scheme 6a will be favored. The strong OHO hydrogen bond formed between the carboxylic group and the phenolic oxygen will shift the phenolic proton to the Schiff base nitrogen in a manner similar to the protonation of the pyridine ring.

Some evidence for the formation of the OHO 1:1 complex is obtained by considering the reaction depicted in Scheme 6b. An OHN 1:1 complex of aspartic acid with internal aldimine will not exhibit a secondary Asp–Asp interaction. The aspartic acid will then prefer to interact with an external aldimine, shifting the equilibrium to the right side. This explains why the enolimine peak is weaker than the ketoenimine peak.

Aldimine Tautomerism. From the limiting ^{15}N chemical shifts of the two tautomeric forms, we calculate the equilibrium constants of tautomerism listed in Table 2 using a simple two-state model that neglects changes in the intrinsic chemical shifts with changing equilibrium constants.[39] The equilibrium constants obtained are up to 0.3 for extensive hydration alone and up to about 18 for the PLP-Asp aldimine in PLL. Two other ^{15}N chemical shifts of PLP enzymatic intermediates were found in the literature and are included in Table 2. The external aldimine of AlaR with ^{15}N-labeled inhibitor (1-aminoethyl)-phosphonic acid studied by Griffin et al.[49] exhibits a chemical shift of 150 ppm, which is slightly larger than that of PLP-Asp. The equilibrium constant is therefore somewhat smaller.

The findings of Mueller et al.[50] are noteworthy. They observed a value of 257.2 ppm for a quinoid complex of tryptophan synthase with aminoacrylate and indoline presented in Scheme 7. On the basis of chemical shift calculations, they interpreted this value in terms of a fast tautomerism between the ketoenamine and enolimine forms (Scheme 7, structures a and b). However, three-site tautomerism involving a partial quinoid form where the adjacent carboxyl group is protonated (Scheme 7, structure c) could not be ruled out. If we assume enolimine–ketoenamine tautomerism, then we obtain an equilibrium constant of about 0.15 (Table 2). In any case, it is clear that the tautomerism found by Mueller et al.[50] is different from that found here or that found by Griffin et al.[49]

Biological Implications. *Acid–Base Behavior in Protein Environments Compared to That in Aqueous Solution.* We have shown that the OHN H-bond between Asp222 and the pyridine nitrogen of PLP in AspAT adopts the same geometry as in the corresponding model system in a polar organic solvent exhibiting a dielectric constant of about 30. This dielectric value is far below that of water; in the interior of a protein, this local polarity is induced mostly by polar side chains and bound water molecules. Thus, the active-site environment is better modeled using proton donors in polar aprotic solvents than in water.

The concept of pK_a values that describe the protonation states of acids and bases in water breaks down in proteins where direct, highly structured, and persistent acid–base H-bonds are formed. At physiological pH, carboxylic acids are deprotonated in water and are present as anions, and nitrogen bases of intermediate strength such as pyridine and histidine are neutral (i.e., not protonated in water). However, if they are brought together to interact in the interior of a protein, then their combined basicity and the active-site environment enable a proton from solution to be bound between them. The individual pK_a values of both species are replaced by an apparent pK_a value of the H-bonded complex formed. This value corresponds to the pH in water where the bond is destroyed by the removal of the proton. The location of H in the H-bond cannot be predicted simply by the pK_a values of the constituent groups in water; rather it depends on the local electrostatics of the enzymatic active site.

Activation of AlaR. We come back to the issue of how the internal aldimine in AlaR might be activated for the initial

dx.doi.org/10.1021/ja408988z | J. Am. Chem. Soc. 2013, 135, 18160–18175

nucleophilic attack by a substrate in the course of transimination. The results presented here imply an important role for a strong H-bond to or protonation of the phenolic oxygen, as illustrated in Scheme 3b. Even partial proton transfer to the phenolic oxygen might provide enough positive charge on the aldimine nitrogen to initiate nucleophilic attack. A strong OHO hydrogen bond could be formed by two water molecules that might contain an additional proton in the uncomplexed enzyme (Scheme 2, structure b), a feature that has not been discussed previously. In other words, O-protonation might be as efficient in the activation of the cofactor as N-protonation. This hypothesis requires further experimental and theoretical study.

Transimination Pathway. Do our studies have implications for the mechanism of transimination, where both a gem-diamine pathway and a hydrolysis pathway are conceivable a priori (Scheme 8)? Jencks et al.[8] and Toney et al.[17] provide good evidence for the existence of a gem-diamine intermediate in model studies and in AspAT, respectively, on the basis of kinetics measurements. Cook et al.[25] observed a gem-diamine intermediate in the crystal structure of GDP-4-keto-6-deoxy-D-mannose-3-dehydratase and using UV−vis spectroscopy, although the protonation state of the gem-diamine could not be determined. In the present solid-state model system of PLP in PLL, we could not find any evidence for the presence of a gem-diamine; moreover, under conditions of reduced mobility, we observed hydrolysis that represents part of the second pathway. We suggest that the gem-diamine pathway requires a particular chemical and conformational environment to promote and stabilize the gem-diamine intermediate, which is not provided by PLL but is provided by PLP-dependent enzymes. This environment juxtaposes the unprotonated nucleophilic amino group with C-4′ of the imine and stabilizes the high-energy gem-diamine intermediate on the pathway to the new aldimine. A still poorly understood aspect of enzymatic transimination is the mechanism by which the proton-transfer steps required to convert the initial gem-diamine to the final imine occur. This could happen via the intrinsic acid/base properties of the phenolic O-3′ oxygen with or without direct facilitation by the enzymatic environment.

Scheme 8. Gem-Diamine and Hydrolysis Pathways for the Transimination Step of PLP-Dependent Enzymes

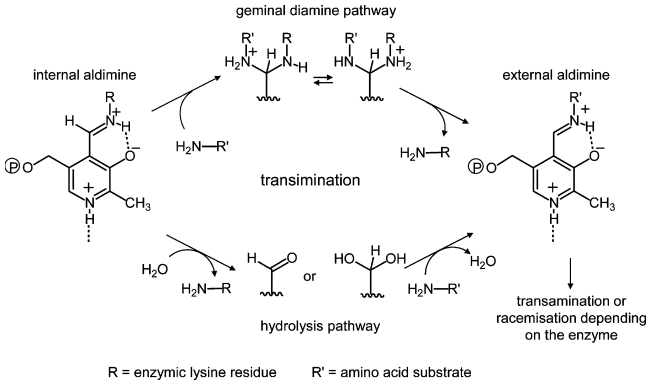

CONCLUSIONS

We arrive at the following conclusions from this study. (i) Using solid-state NMR, we were able to confirm that the pyridine nitrogen of PLP is protonated and involved in a strong H-bond in the case of AspAT but unprotonated and weakly H-bonded in the case of AlaR. (ii) Poly-L-lysine (PLL) is an excellent model environment for the study of the protonation, tautomerism, and H-bonded states of PLP aldimines in a protein like environment because the water and acid contents can be easily controlled. In this medium, we reproduced the ^{15}N chemical shifts of the pyridine nitrogens of AspAT and AlaR and hence the properties of the corresponding H-bonds, in particular, their mutual coupling. In addition, we obtained evidence for the formation of a 1:1 complex between free aspartic acid and an external aldimine via the formation of a strong OHO hydrogen bond to the phenolic oxygen. (iii) The formation of a strong OHO hydrogen bond to the phenolic oxygen or full O-protonation activates the cofactor by shifting the phenolic proton toward the Schiff base nitrogen in a similar way as does protonation of the pyridine ring (Scheme 3). We propose that this hypothesis might explain the activation of AlaR for external aldimine formation. The observed stability of the hydrated PLP−PLL in water at neutral pH and the formation of the ketoenamine tautomer at high pH show that the activation of PLP for transimination in AlaR cannot be explained simply by interaction with solvent dipoles. (iv) The gem-diamine pathway of the transimination reaction is energetically not favored compared to the hydrolysis pathway in an environment such as poly-L-lysine. In the latter, aldimine hydrolysis required the addition of acid followed by hydration. In PLP-dependent enzymes, transimination via a gem-diamine intermediate is enforced by the substrate amino group and the internal aldimine being apposed in a precise manner. Enzymes further facilitate direct transimination by providing conditions of stabilizing a net positive charge on the aldimine nitrogen, either by protonating the pyridine nitrogen or by directly stabilizing the negative charge on the 3′ oxygen.

ASSOCIATED CONTENT

Supporting Information

Preparation and characterization of ^{15}N-PLL$_l$, acquisition parameters of the NMR spectra shown in the main text, and ^{15}N CPMAS spectra of a 1:1 mixture of ^{15}N-PLL$_h$ with PLP lyophilized from aqueous solutions at different pH values. This material is available free of charge via the Internet at http://pubs.acs.org.

AUTHOR INFORMATION

Corresponding Authors

limbach@chemie.fu-berlin.de
chanhuot.monique@gmail.com

Notes

The authors declare no competing financial interest.

ACKNOWLEDGMENTS

We thank the Deutsche Forschungsgemeinschaft, Bonn (Li300/25-1) and the Russian Foundation of Basic Research (projects 11-03-00346 and 11-03-00237) for financial support.

REFERENCES

(1) Toney, M. D. *Biochim. Biophys. Acta* **2011**, *1814*, 1405−1406.
(2) Christen, P.; Metzler, D. E. *Transaminases*; John Wiley & Sons: New York, 1985; pp 37−101.
(3) Spies, M. A.; Toney, M. D. *Biochemistry* **2003**, *42*, 5099−5107.
(4) Malashkevich, V. N.; Toney, M. D.; Jansonius, J. N. *Biochemistry* **1993**, *32*, 13451−13462.
(5) Zhou, X.; Toney, M. D. *Biochemistry* **1998**, *38*, 311−320.

(6) Chan-Huot, M.; Sharif, S.; Tolstoy, P. M.; Toney, M. D.; Limbach, H. H. *Biochemistry* **2010**, *49*, 10818−10830.
(7) Metzler, D. E. *Biochemistry: The Chemical Reactions of Living Cells*; Academic Press: New York, 1977, Vol. *1*, pp 444−461.
(8) Cordes, E. H.; Jencks, W. P. *Biochemistry* **1962**, *1*, 773−778.
(9) Snell, E. E.; Jenkins, W. T. *J. Cell. Comput. Physiol. 1* **1959**, *54*, 161−177.
(10) Tobias, P. S.; Kallen, R. G. *J. Am. Chem. Soc.* **1975**, *97*, 6530−6539.
(11) Schirch, L. *J. Biol. Chem.* **1975**, *250*, 1939−1945.
(12) Ulévitch, R. J.; Kallen, R. G. *Biochemistry* **1977**, *16*, 5355−5363.
(13) Fischer, H.; De Candis, F. X.; Ogden, D.; Jencks, W. P. *J. Am. Chem. Soc.* **1980**, *102*, 1340−1347.
(14) Korpela, T.; Mäkelä, M.; Lönnberg, H. *Arch. Biochem. Biophys.* **1981**, *212*, 581−588.
(15) Vázquez, M. A.; Muñoz, F.; Donoso, J. *J. Phys. Org. Chem.* **1992**, *5*, 142−154.
(16) (a) Drewe, W. F., Jr.; Dunn, M. F. *Biochemistry* **1985**, *24*, 3977−3987. (b) Drewe, W. F., Jr.; Dunn, M. F. *Biochemistry* **1986**, *25*, 2494−2501.
(17) Toney, M. D.; Kirsch, J. F. *Biochemistry* **1993**, *32*, 1471−1479.
(18) Salvà, A.; Donoso, S.; Frau, J.; Munoz, F. *J. Phys. Chem. A* **2004**, *108*, 11709−11714.
(19) Barbolina, M. V.; Phillips, R. S.; Gollnick, P. D.; Faleev, N. G.; Demidkina, T. V. *Protein Eng.* **2000**, *13*, 207−215.
(20) Sivaraman, J.; Li, Y.; Larocque, R.; Schrag, J. D.; Cygler, M.; Matte, A. *J. Mol. Biol.* **2001**, *311*, 761−776.
(21) Jhee, K. H.; Niks, D.; McPhie, P.; Dunn, M. F.; Miles, E. W. *Biochemistry* **2001**, *40*, 10873−10880.
(22) Phillips, R. S.; Demidkina, T. V.; Zakomirdina, L. N.; Bruno, S.; Ronda, L.; Mozzarelli, A. *J. Biol. Chem.* **2002**, *277*, 21592−21597.
(23) Karthikeyan, S.; Zhou, Q.; Zhao, Z.; Kao, C. L.; Tao, Z.; Robinson, H.; Liu, H. W.; Zhang, H. *Biochemistry* **2004**, *43*, 13328−13339.
(24) Jackson, L. K.; Baldwin, J.; Akella, R.; Goldsmith, E. J.; Phillips, M. A. *Biochemistry* **2004**, *43*, 12990−12999.
(25) Cook, P. D.; Holden, H. M. *Biochemistry* **2007**, *46*, 14215−14224.
(26) Jo, B. H.; Nair, V.; Davis, L. *J. Am. Chem. Soc.* **1977**, *99*, 4467−4471.
(27) Hershey, S.; Leussing, D. L. *J. Am. Chem. Soc.* **1977**, *99*, 1992−1993.
(28) Bach, R. D.; Canepa, C. *J. Am. Chem. Soc.* **1997**, *119*, 11725−11733.
(29) Snell, E. E.; Di Mari, S. J. *The Enzymes*, 3rd ed.; Boyer, P. D., Ed.; Academic Press: New York, 1970; Vol. *2*, pp 335−362.
(30) Snell, E. E.; Jenkins, W. T. *J. Cell. Comp. Physiol.* **1959**, *54* (Supp. 1), 161−177.
(31) (a) Mollova, E. T.; Metzler, D. E.; Kintanar, A.; Kagamiyama, H.; Hayashi, H.; Hirotsu, K.; Miyahara, I. *Biochemistry* **1997**, *36*, 615−625. (b) Metzler, D. E.; Metzler, C. M.; Scott, R. D.; Mollova, E. T.; Kagamiyama, H.; Yano, T.; Kuramitsu, S.; Hayashi, H.; Hirotsu, K.; Miyahara, I. *J. Biol. Chem.* **1994**, *269*, 28027−28033. (c) Metzler, D. E.; Metzler, C. M.; Mollova, E. T.; Scott, R. D.; Tanase, S.; Kogo, K.; Higaki, T.; Morino, Y. *J. Biol. Chem.* **1994**, *269*, 28017−28026. (d) Metzler, C. M.; Metzler, D. E.; Kintanar, A.; Scott, R. D.; Marceau, M. *Biochem. Biophys. Res. Commun.* **1991**, *178*, 385−392.
(32) Limbach, H. H.; Denisov, G. S.; Golubev, N. S. In *Isotope Effects in the Biological and Chemical Sciences*; Kohen, A., Limbach, H. H., Eds.; Taylor & Francis: Boca Raton FL, 2005; Chapter 7, pp 193−230.
(33) Limbach, H. H. In *Hydrogen Transfer Reactions*; Hynes, J. T., Klinman, J., Limbach, H. H., Schowen, R. L., Eds.; Wiley-VCH: Weinheim, Germany, 2006; Vols. *1 and 2*, Chapter 6, pp 135−221, and references cited therein.
(34) Sharif, S.; Chan-Huot, M.; Tolstoy, P. M.; Toney, M. D.; Jonsson, K. H. M.; Limbach, H. H. *J. Phys. Chem. B* **2007**, *111*, 3869−3876.
(35) Chan-Huot, M.; Niether, C.; Sharif, S.; Tolstoy, P. M.; Toney, M. D.; Limbach, H. H. *J. Mol. Struct.* **2010**, *976*, 282−289.
(36) Sharif, S.; Powell, D. R.; Schagen, D.; Steiner, T.; Toney, M. D.; Fogle, E.; Limbach, H. H. *Acta Crystallogr.* **2006**, *B62*, 480−487.
(37) Sharif, S.; Schagen, D.; Toney, M. D.; Limbach, H. H. *J. Am. Chem. Soc.* **2007**, *129*, 4440−4455.
(38) Sharif, S.; Denisov, G. S.; Toney, M. D.; Limbach, H. H. *J. Am. Chem. Soc.* **2006**, *128*, 3375−3387.
(39) Sharif, S.; Denisov, G. S.; Toney, M. D.; Limbach, H. H. *J. Am. Chem. Soc.* **2007**, *129*, 6313−6327.
(40) (a) Jansonius, J. N. *Curr. Opin. Struct. Biol.* **1998**, *8*, 759−769. (b) Jager, J.; Moser, M.; Sauder, U.; Jansonius, J. N. *J. Mol. Biol.* **1994**, *239*, 285−305.
(41) (a) Kirsch, J. F.; Eliot, A. C. *Annu. Rev. Biochem.* **2004**, *73*, 383−415. (b) Onuffer, J. J.; Kirsch, J. F. *Protein Eng.* **1994**, *7*, 413−424. (c) Yano, T.; Hinoue, Y.; Chen, V. J.; Metzler, D. E.; Miyahara, I.; Hirotsu, K.; Kagamiyama, H. *J. Mol. Biol.* **1993**, *234*, 1218−1229. (d) Yano, T.; Kuramitsu, S.; Tanase, S.; Morino, Y.; Kagamiyama, H. *Biochemistry* **1992**, *31*, 5878−5887.
(42) Sharif, S.; Fogle, E.; Toney, M. D.; Denisov, G. S.; Shenderovich, I. G.; Tolstoy, P. M.; Chan-Huot, M.; Buntkowsky, G.; Limbach, H. H. *J. Am. Chem. Soc.* **2007**, *129*, 9558−9559.
(43) Bundi, A.; Wüthrich, K. *Biopolymers* **1979**, *18*, 285−297.
(44) Limbach, H. H.; Chan-Huot, M.; Sharif, S.; Tolstoy, P. M.; Shenderovich, I. G.; Denisov, G. S.; Toney, M. D. *Biochim. Biophys. Acta* **2011**, *1814*, 1426−1437.
(45) Barreteau, H.; Kovac, A.; Boniface, A.; Sova, M.; Gobec, S.; Blanot, D. *FEMS Microbiol. Rev.* **2008**, *32*, 168−207.
(46) (a) Shaw, J. P.; Petsko, G. A.; Ringe, D. *Biochemistry* **1997**, *36*, 1329−1342. (b) Morollo, A. A.; Petsko, G. A.; Ringe, D. *Biochemistry* **1999**, *38*, 3293−3301.
(47) Au, K.; Ren, J.; Walter, T. S.; Harlos, K.; Nettleship, J. E.; Owens, R. J.; Stuart, D. I.; Esnouf, R. M. *Acta Crystallogr.* **2008**, *F64*, 327−333.
(48) (a) Major, D. T.; Nam, K.; Gao, J. *J. Am. Chem. Soc.* **2006**, *128*, 16345−16357. (b) Major, D. T.; Nam, K.; Gao, J. *J. Am. Chem. Soc.* **2006**, *128*, 8114−8115. (c) Lin, Y. L.; Gao, J. *Biochemistry* **2010**, *49*, 84−94. (d) Lin, Y. L.; Gao, J.; Rubinstein, A.; Major, D. T. *Biochim. Biophys. Acta* **2011**, *1814*, 1438−1446.
(49) Copié, V.; Faraci, W. S.; Walsh, C. T.; Griffin, R. G. *Biochemistry* **1988**, *27*, 4966−4970.
(50) Lai, J.; Niks, D.; Wang, Y.; Domratcheva, T.; Barends, T. R. M.; Schwarz, F.; Olsen, R. A.; Elliott, D. W.; Fatmi, M. Q.; Chang, C. A.; Schlichting, I.; Dunn, M. F.; Mueller, L. J. *J. Am. Chem. Soc.* **2011**, *133*, 4−7.
(51) (a) Dos, A.; Schimming, V.; Tosoni, S.; Limbach, H. H. *J. Phys. Chem. B* **2008**, *112*, 15604−15615. (b) Dos, A.; Schimming, V.; Chan-Huot, M.; Limbach, H. H. *J. Am. Chem. Soc.* **2009**, *131*, 7641−7653. (c) Dos, A.; Schimming, V.; Chan-Huot, M.; Limbach, H. H. *Phys. Chem. Chem. Phys.* **2010**, *12*, 10235−10245.
(52) Griswold, W. R.; Fisher, A. J.; Toney, M. D. *Biochemistry* **2011**, *50*, 5918−5924.
(53) Sun, S.; Toney, M. D. *Biochemistry* **1999**, *38*, 4058−4065.
(54) Hernandez, J. R.; Klok, H. A. *J. Polym. Sci., Part A: Polym. Chem.* **2003**, *41*, 1167−1187.
(55) Schimming, V.; Hoelger, C. G.; Buntkowsky, G.; Sack, I.; Fuhrhop, J. H.; Rocchetti, S.; Limbach, H. H. *J. Am. Chem. Soc.* **1999**, *121*, 4892−4893.
(56) Hayashi, S.; Hayamizu, K. *Bull. Chem. Soc. Jpn.* **1991**, *64*, 688−690.
(57) Wishart, D. S.; Bigam, C. G.; Sykes, B. D. *J. Biomol. NMR* **1995**, *6*, 135−140.
(58) (a) Lorente, P.; Shenderovich, I. G.; Buntkowsky, G.; Golubev, N. S.; Denisov, G. S.; Limbach, H. H. *Magn. Reson. Chem.* **2001**, *39*, S18−S29. (b) Limbach, H. H.; Pietrzak, M.; Sharif, S.; Tolstoy, P. M.; Shenderovich, I. G.; Smirnov, S. N.; Golubev, N. S.; Denisov, G. S. *Chem.—Eur. J.* **2004**, *10*, 5195−5204. (c) Ip, B. C. K.; Shenderovich, I. G.; Tolstoy, P. M.; Frydel, J.; Denisov, G. S.; Buntkowsky, G.; Limbach, H. H. *J. Phys. Chem. A* **2012**, *116*, 11370−11387.

(59) Tolstoy, P.; Guo, J.; Koeppe, B.; Golubev, N.; Denisov, G.; Smirnov, S.; Limbach, H. H. *J. Phys. Chem. A* **2010**, *114*, 10775−10782.
(60) Shenderovich, I. G.; Burtsev, A. P.; Denisov, G. S.; Golubev, N. S.; Limbach, H. H. *Magn. Reson. Chem.* **2001**, *39*, S91−S99.
(61) (a) Golubev, N. S.; Smirnov, S. N.; Gindin, V. A.; Denisov, G. S.; Benedict, H.; Limbach, H. H. *J. Am. Chem. Soc.* **1994**, *116*, 12055−12056. (b) Smirnov, S. N.; Golubev, N. S.; Denisov, G. S.; Benedict, H.; Schah-Mohammedi, P.; Limbach, H. H. *J. Am. Chem. Soc.* **1996**, *118*, 4094−4101. (c) Tolstoy, P. M.; Smirnov, S. N.; Shenderovich, I. G.; Golubev, N. S.; Denisov, G. S.; Limbach, H. H. *J. Mol. Struct.* **2004**, *700*, 19−27.
(62) Kricheldorf, H. R.; Müller, D. *Macromolecules* **1983**, *16*, 615−623.
(63) (a) Wehrle, B.; Zimmermann, H.; Limbach, H. H. *J. Am. Chem. Soc.* **1988**, *110*, 7014−7024. (b) Wehrle, B.; Limbach, H. H. *Chem. Phys.* **1989**, *136*, 223−247.
(64) Golubev, N. S.; Smirnov, S. N.; Tolstoy, P. M.; Sharif, S.; Toney, M. D.; Denisov, G. S.; Limbach, H. H. *J. Mol. Struct.* **2007**, *844*−*845*, 319−327.